applied sciences

MDPI

Article

An Analytical Solution for the Deformation of Soft Ground Reinforced by Columnar Inclusions under Equal Stress Conditions

Zan Zhou [1], Thomas Man-Hoi Lok [1,*], Wan-Huan Zhou [1] and Lin-Shuang Zhao [2]

[1] Department of Civil and Environmental Engineering, Faculty of Science and Technology, University of Macau, Macau 999078, China
[2] Department of Civil and Environmental Engineering, College of Engineering, Shantou University, Shantou 515000, China
* Correspondence: mhlok@um.edu.mo; Tel.: +(853)-8322-4366

Abstract: Columnar inclusion is a versatile and cost-effective technique for improving weak soils. Currently, most approaches are based on the "equal strain" assumption to calculate the deformation of soft ground reinforced by columnar inclusions. In this study, a new model to simulate the behavior of column-reinforced soft soil under equal stress conditions based on the variational principles is proposed. The proposed model satisfies the force equilibrium and deformation compatibility simultaneously, which is seldom fulfilled in traditional empirical methods or other analytical models. The corresponding analytical solution is obtained and its accuracy is verified by comparing it with the numerical solutions using finite element analysis. The comparisons of the proposed solution with an existing solution show that the proposed solution can provide very close agreement over a wide range of parameters while the existing solution is only able to provide a reasonable agreement for a certain range of stiffness ratio of the column and soft ground. In addition, a parametric study is made to illustrate the influence of various parameters on ground settlement predictions. The parametric study indicated that, by increasing the ratio of elastic modulus between the stone column and surrounding soils and the ratio between the radius of the stone column and the space of the stone column, the load transfer effect has been significantly improved, and the ground settlement becomes smaller. Furthermore, the Poisson's ratio of the surrounding soil also has a very significant effect on ground settlement, while the effect of the Poisson's ratio of the stone column on ground settlement is less significant compared with that of the surrounding soil.

Keywords: analytical solution; ground settlement; variational principles; column-reinforced foundation

Citation: Zhou, Z.; Lok, T.M.-H.; Zhou, W.-H.; Zhao, L.-S. An Analytical Solution for the Deformation of Soft Ground Reinforced by Columnar Inclusions under Equal Stress Conditions. *Appl. Sci.* **2022**, *12*, 11574. https://doi.org/10.3390/app122211574

Academic Editor: Chin Leo

Received: 23 September 2022
Accepted: 24 October 2022
Published: 15 November 2022

1. Introduction

Soil improvement is becoming increasingly important due to the lack of quality land for the development of structures and transport infrastructure [1–4], and at the same time, the need for rapid construction of embankments for highways and railways over soft ground [5–8]. There are various methods of soil improvement, and among these methods, columnar inclusion is one of the most effective techniques [8,9]. The columnar inclusions such as stone columns, sand compaction piles, jet grout columns, etc., are common and efficient techniques to improve the soft and weak ground with low bearing capacity, high compressibility, and large settlement [10,11]. Previous studies have shown that columnar inclusions can significantly enhance the bearing capacity [12–16], reduce the amount of settlement [17,18], accelerate consolidation [19,20], improve slope stability [21], and avoid liquefaction of soil [22–24].

The role of columnar inclusion in limiting settlement is essential in some cases, for example, road embankments and land reclamations. Many theoretical or semi-empirical approaches have been proposed to study the behavior of column-reinforced foundations

and to evaluate ground settlement [25]. The simplest analytical approach to columnar inclusion is known as the "equilibrium method". This approach is based on elasticity theory and has been depicted by Aboshi et al. [26]; it assumes that vertical equilibrium between the columns and the soils satisfied vertical equilibrium with oedometric conditions in the soil and ignores the axial friction was ignored [27]. Furthermore, Balaam and Booker [28] proposed a method that can be used to get a closed-form analytical solution. Subsequently, Balaam and Booker [29] proposed an iterative approach that requires a numerical implementation to obtain a solution. Based on a semi-experiential approach, Priebe [30] developed one of the most popular design methods in European practice to estimate the settlement of subsoil reinforced with an end-bearing stone column. In addition, Pulko and Majes [31] proposed an analytical method to analyze the behavior of rigid foundations resting on soft soil stabilized by a large number of end-bearing stone columns. Zhang et al. [32] proposed an analytical solution to calculate the deformation of the composite foundations reinforced with stone columns by considering the radial expansion of the stone column among the surrounding soil near the top portion of the column. However, these methods can only provide results with equal vertical strain based on the "equal strain" assumption. For the case with different vertical strains, the approaches with the "equal strain" assumption cannot provide the actual behavior of the column-reinforced foundations. Zhao et al. [33] indicated that, for the column-reinforced embankment, the deformations of the stone column and surrounding soil are different, and cannot be described by the "equal strain" assumption.

Alamgir et al. [34] first paid attention to this problem and provided the deformation analysis on the reinforced foundation with columnar inclusion subjected to a uniform surcharge. The deformation field proposed by Alamgir et al. was used by many following researchers to study the behavior of column-reinforced foundations. In particular, Deb and Mohapatra [35] and Zhao et al. [33,36] adopted Alamgir et al.'s solution for the deformation of the reinforced foundation to analyze the column-supported embankment, taking into account the effect of soil arching from the embankment. The analytical method of Alamgir et al. provided a technique to consider the effects of the column modulus on the settlement process and the stress distribution on the ground surface, which provide useful information for further analysis of soil arching in the embankment. However, the deformation pattern of the reinforced foundation in Alamgir et al. was assumed to follow a certain shape function, from which strain and stress were derived. Comparison of the settlement predicted by this method with finite element analysis was satisfactory for certain values of column modulus. However, it was found by further investigations that the predicted settlement may be very different from finite element analysis in certain situations.

The reason for the shortcomings of Alamgir et al.'s solution is that an empirical function assumption was assumed for the deformation of the foundation soil. To overcome the above drawbacks, a rigorous analytical solution needs to be proposed. In this study, a rigorous analytical solution is proposed for the deformation of column-reinforced foundations under equal stress conditions. Unlike Alamgir et al.'s approach, in which a deformation shape function is assumed empirically, the proposed solution is derived based on the variational principles. Therefore, the proposed solution satisfies the equilibrium and compatibility conditions simultaneously and provides a more accurate deformation pattern of the composite foundation. Finite element analyses are first performed to verify the accuracy of the proposed solution. The solution is then compared with the physical observations of a previous experimental study. A detailed parametric study is then carried out using the proposed solution for the behavior of column-reinforced foundation over a wide range of column modulus and spacing.

2. Model Formulation and Analysis

A general situation for column-reinforced foundations is shown in Figure 1a. It is assumed that a uniform load is applied at the ground surface. The columnar inclusions are installed in the soft ground and rest on the bedrock which is assumed to be a rigid

base. The columns of radius r_c are arranged in a square pattern with spacing s as shown in Figure 1b.

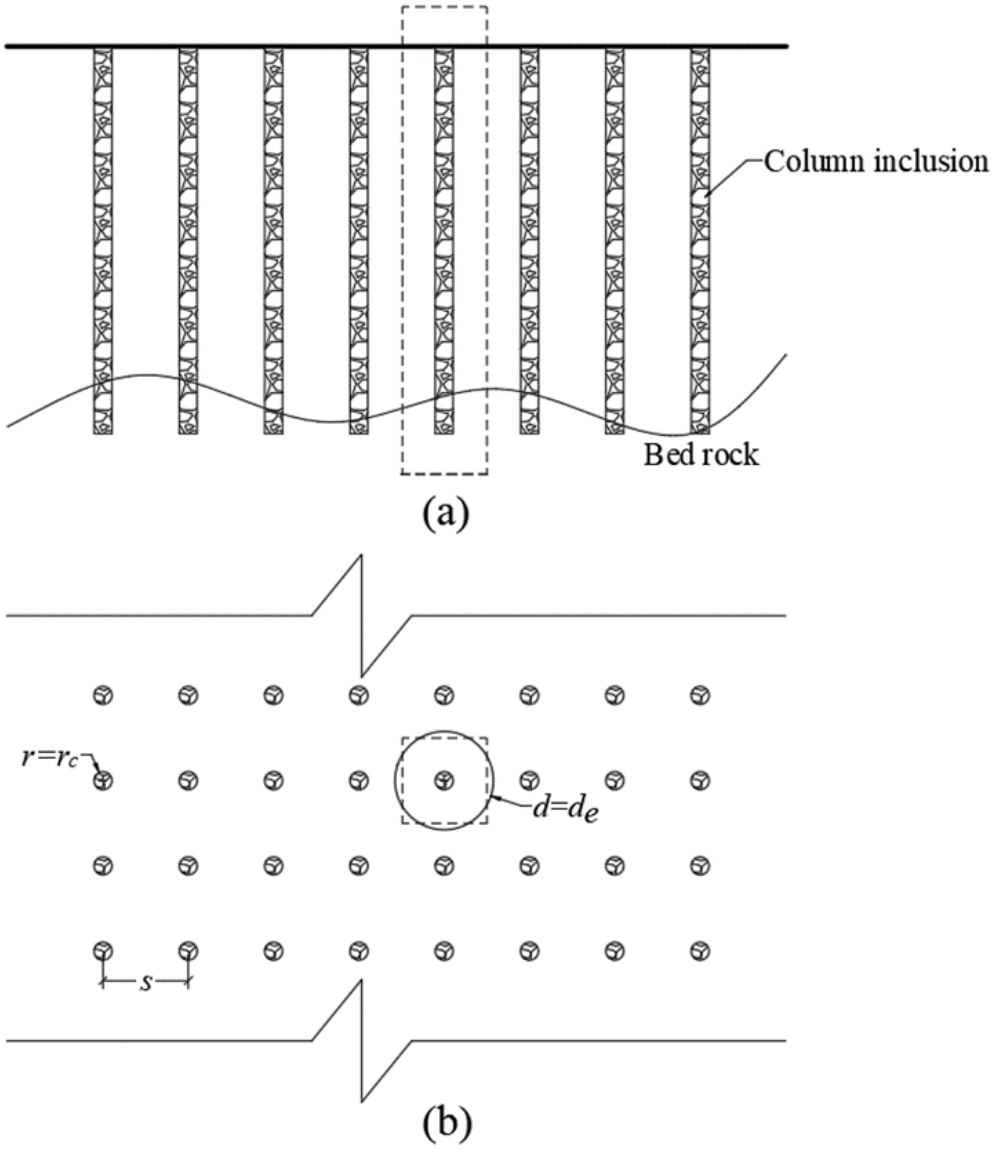

Figure 1. General situation of column-reinforced foundation system: (**a**) side view, (**b**) top view.

The behavior of the column-reinforced foundation is generally represented by a cylindrical unit cell containing a single column with surrounding soil as shown in Figures 1b and 2. Based on the equivalence of contributory area, the equivalent diameter, d_e, of the unit cell is given as:

$$d_e = k \cdot s \tag{1}$$

where s is the spacing of the columns, and k is a constant that depends on the arrangement pattern of the columns. k is equal to 1.05, 1.13, and 1.29 for a triangular, square, and hexagonal pattern of columns, respectively [28].

2.1. Existing Solution for Deformation Analysis of the Column-Reinforced Foundation

Alamgir et al. [34] proposed a procedure to analyze the deformation of the column-reinforced foundation by assuming a deformation shape function for the surrounding soil as follows:

$$w(r,z) = w_c(z) + \alpha_c(z)\left[\frac{r}{r_c} - \exp\beta_c\left(\frac{r}{r_c} - 1\right)\right] \tag{2}$$

where $w(r,z)$ is the surrounding soil deformation at depth z and radial distance r. $w_c(z)$ is the deformation of the column at depth z. r_c is the diameter of the column. $\alpha_c(z)$ are the deformation parameters to be determined as described by Alamgir et al. using the boundary conditions such as the zero shear stress at the outside boundary and the deformation compatibility of the soil and the column. The resulting deformation shape is shown in Figure 3.

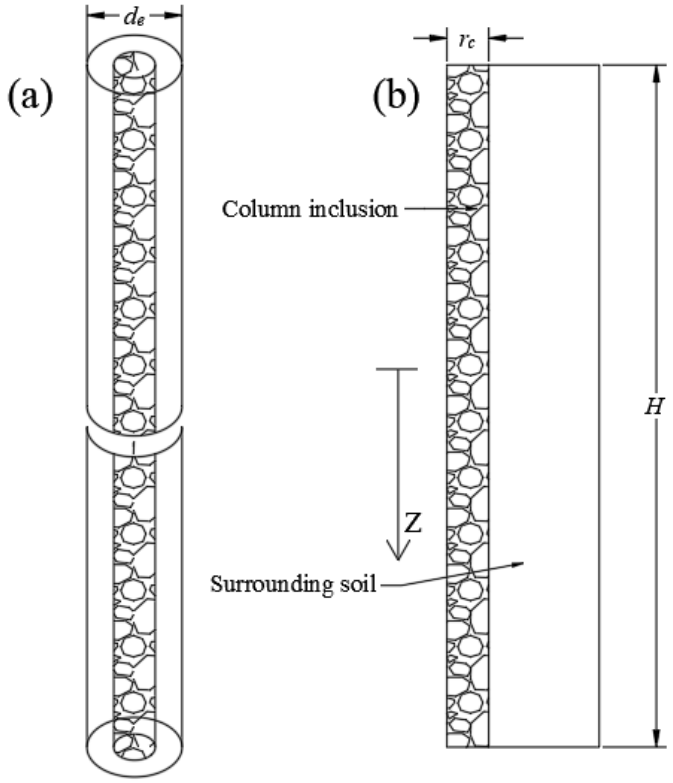

Figure 2. Unit cell of soft soil foundation reinforced by columnar inclusions: (**a**) sketch of a unit cell, (**b**) one cross-section of the unit cell.

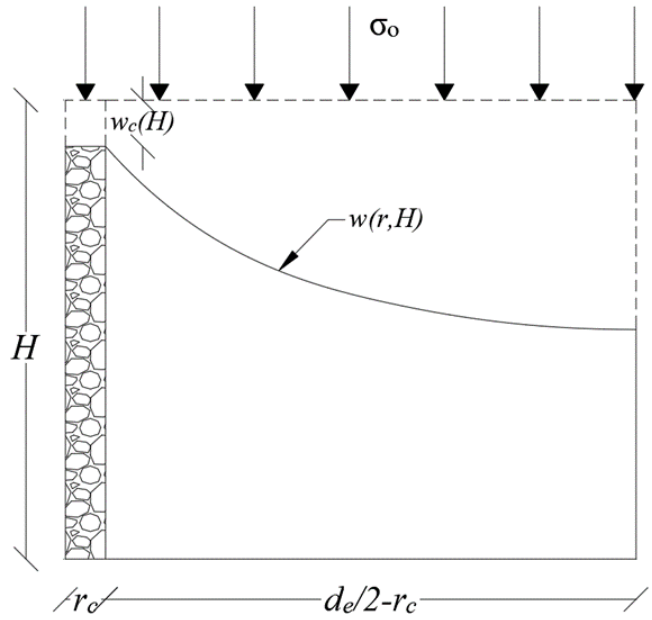

Figure 3. The assumed deformation shape, by Alamgir et al. [34].

2.2. Mathematical Modeling

The solution proposed by Alamgir et al. [34] is important for providing the settlement profile at the ground surface of the column-reinforced foundation. However, the limitation is that this solution relies on the assumed deformation shape function, which was constructed using simple functions. Therefore, the solution does not satisfy the stress equilibrium condition of the model. To overcome this limitation, an improved solution is proposed by using the variational principles, for which the deformation shape is obtained naturally. In addition, the equilibrium condition is also ensured by the variational principles.

In this study, the soil is assumed to behave as a linearly elastic homogeneous continuum, with a constant modulus E_s and a constant Poisson's ratio ν_s, unaffected by the presence of columns, and remaining unchanged throughout the loading process. It is also assumed that the column material behaves as a linearly elastic homogeneous material with a deformation modulus E_c and a constant Poisson's ratio ν_c. Furthermore, it is assumed that the interface between soil and column remains intact and does not slip, and the displacements of the column and the soil at the interface are equal. Since the unit cell is symmetric, only half of the model is considered in the analysis, as shown in Figure 4 in which the depth is equal to H and the radius of the column is r_c. The radius of the entire model is $d_e/2$, which is determined by Equation (1) with the spacing of the columns, s, based on the area equivalence assumption.

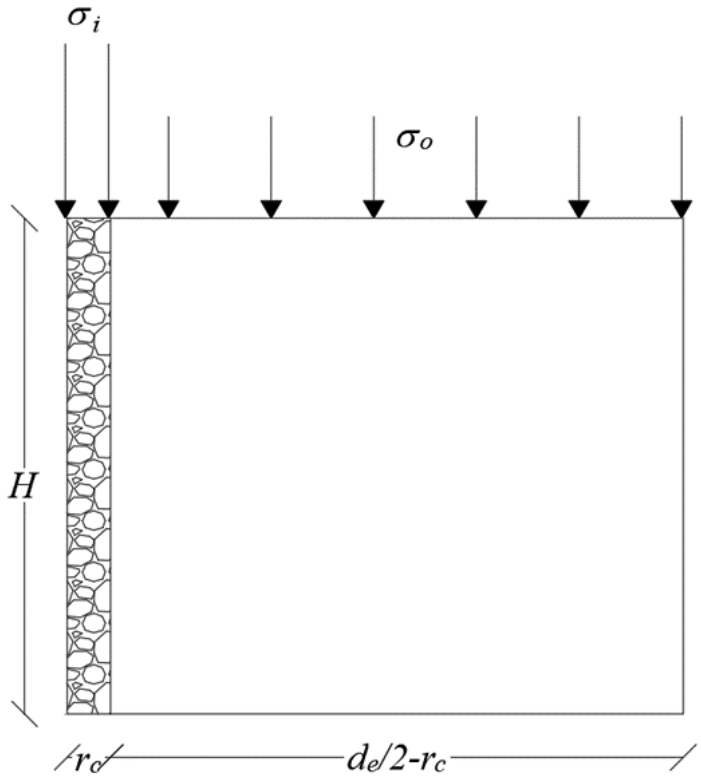

Figure 4. Axisymmetric model of the column-reinforced foundation.

When the stress, σ_i, is applied to the column, and the stress, σ_o, is applied to the surrounding soil, the column-reinforced soil starts to deform. As linear elastic behavior is assumed, the total potential energy Π of the entire system can be introduced as

$$\Pi = \prod_c + \int_{r_c}^{\frac{d_e}{2}} \int_0^{2\pi} \int_0^{H} \frac{1}{2}(\sigma_z \varepsilon_z + \sigma_r \varepsilon_r + \tau_{rz}\gamma_{rz}) r dr dz d\theta - \int_0^{2\pi} \int_{r_c}^{\frac{d_e}{2}} \sigma_o W(r,0) r dr d\theta \quad (3)$$

where Π_c is the total energy of column inclusion, including the internal and external energy, and σ_z, σ_r, τ_{rz}, ε_z, ε_r, γ_{rz} are the stresses and corresponding strains of a small element of the soil continuum. $W(r, 0)$ is the vertical displacement at the surface of the surrounding soil at the location of $(r, 0)$ in the cylindrical coordinate system.

The constitutive equations in an axisymmetric condition can be written as

$$\begin{pmatrix} \sigma_{\mathrm{r}} \\ \sigma_\theta \\ \sigma_z \\ \tau_{rz} \end{pmatrix} = \frac{(1-\nu)E}{(1+\nu)(1-2\nu)} \begin{bmatrix} 1 & \frac{\nu}{1-\nu} & \frac{\nu}{1-\nu} & 0 \\ \frac{\nu}{1-\nu} & 1 & \frac{\nu}{1-\nu} & 0 \\ \frac{\nu}{1-\nu} & \frac{\nu}{1-\nu} & 1 & 0 \\ 0 & 0 & 0 & \frac{1-2\nu}{2(1-\nu)} \end{bmatrix} \begin{pmatrix} \varepsilon_r \\ \varepsilon_\theta \\ \varepsilon_z \\ \tau_{rz} \end{pmatrix} \tag{4}$$

Because the peripheral displacement equals zero due to the axisymmetric condition, the corresponding strain can be described as

$$\varepsilon_r = \frac{\partial u(r,z)}{\partial r}, \varepsilon_\theta = \frac{u(r,z)}{r}, \varepsilon_z = \frac{\partial W(r,z)}{\partial z}, \gamma_{rz} = \frac{\partial u(r,z)}{\partial z} + \frac{\partial W(r,z)}{\partial r} \tag{5}$$

where $u(r,z)$ and $W(r,z)$ represent the radial displacement and the vertical displacement, respectively.

To simplify the analysis, the following assumptions are adopted [37].

(1) The radial displacement u is assumed to be equal to zero everywhere throughout the soil column model. Because the radial displacement is negligible compared to the vertical displacement under vertical load conditions.

(2) The vertical displacement of the surrounding soil W is expressed by the vertical surface displacement $w(r)$ and the shape function $\phi(z)$ as

$$W(r,z) = w(r)\phi(z) \tag{6}$$

where the boundary conditions can be assumed as $\phi(0) = 1$ and $\phi(H) = 0$.

Inserting Equations (6) and (4) into Equation (3) yields the following equation:

$$\begin{aligned} \Pi = \Pi_c + \int_{r_c}^{\frac{d_e}{2}} \int_0^{2\pi} \int_0^H \left[\begin{array}{c} \frac{(1-\nu_s)E_s}{2(1+\nu_s)(1-2\nu_s)} \left(\frac{d\phi}{dz}\right)^2 w^2 \\ + \frac{E_s}{4(1+\nu_s)} \phi^2 \left(\frac{dw}{dr}\right)^2 \end{array} \right] dz d\theta r dr \\ - \int_0^{r_c} \int_0^{2\pi} \sigma_0 w d\theta r dr \end{aligned} \tag{7}$$

By minimizing the function Π with respect to $\boldsymbol{w}$ based on the variational principles, the following governing equation is obtained.

$$kw - G\left(\frac{d^2w}{dr^2} + \frac{1}{r}\frac{dw}{dr}\right) = \sigma_o \quad r_c \le r \le \frac{d_e}{2} \tag{8}$$

where

$$\begin{cases} k = \frac{(1-\nu_s)E_s}{(1+\nu_s)(1-2\nu_s)} \int_0^H \left(\frac{d\phi}{dz}\right)^2 dz \\ G = \frac{E_s}{2(1+\nu_s)} \int_0^H \phi^2 dz \end{cases} \tag{9}$$

By minimizing the total potential energy Π of Equation (7) with respect to ϕ, the following equation is obtained:

$$-m\frac{d^2\phi}{dz^2} + n\phi = 0 \tag{10}$$

where

$$\begin{cases} m = \frac{(1-\nu_s)E_s}{(1+\nu_s)(1-2\nu_s)} \int_{r_c}^{\frac{d_e}{2}} w^2 r dr \\ n = \frac{E_s}{2(1+\nu_s)} \int_{r_c}^{\frac{d_e}{2}} \left(\frac{dw}{dr}\right)^2 r dr \end{cases} \tag{11}$$

By introducing a new parameter η, the following equation can be obtained:

$$\frac{n}{m} = \left(\frac{\eta}{H}\right)^2 \tag{12}$$

Substitute Equation (12) into Equation (10), and the following equation can be derived:

$$\frac{d^2\phi}{dz^2} - \left(\frac{\eta}{H}\right)^2 \phi = 0 \tag{13}$$

Equation (11) implies that m and n depend on the surface displacement function $\boldsymbol{w}$. At the same time, w depends on the variable η. Therefore, the surface function $\boldsymbol{w}$ and shape function $\boldsymbol{\phi}$ are coupling together. To uncouple these functions, Vallabhan et al. [38] proposed an iterative method to solve Equations (8) and (12) simultaneously.

Jones et al. [39] solved Equation (13) with the boundary conditions $\phi(0) = 1$ and $\phi(H) = 0$, then revealed that the solution is the shape function in Equation (14).

$$\phi(z) = \frac{\sinh[\eta(1 - z/H)]}{\sinh(\eta)} \tag{14}$$

Equation (14) is a general form for $\phi(z)$, and Vlasov et al. [40] proposed an approximate form of the shape function $\phi(z)$ in a thin layer as follows:

$$\phi(z) = 1 - z/H \tag{15}$$

According to Equation (8), the function, $w(r)$, is the solution for a second-order variable coefficient differential equation, which consists of two parts, namely the homogeneous solution and the specific solution. The homogeneous solution is given by the Bessel function, which can be readily obtained. For the specific solution, the constant $\frac{\sigma_0}{k}$ satisfies this equation. Therefore, its general solution is derived as

$$\begin{cases} w(r) = C_1 K_0(a \times r) + C_2 I_0(a \times r) + \frac{\sigma_0}{k} \\ a = \sqrt{\frac{k}{G}} \end{cases} \tag{16}$$

where I_0 and K_0 are the zero-order modified Bessel functions of the first and the second kind, respectively. Only the deformation of the surrounding soil is considered in the above-derived solution. On the other hand, the columnar inclusion also has deformation, which is related to the deformation of the surrounding soil.

For the columnar inclusion, a unit cell is selected and the free body diagram for an infinitesimal element is shown in Figure 5. From this figure, the differential equation of columnar inclusion can be written as follows:

$$\begin{cases} \pi r_c^2(\sigma_c + \mathrm{d}\sigma_c - \sigma_c) = 2\pi \mathrm{r}_c \tau_{rz} dz \\ \gamma_{rz} = \phi \frac{dw}{dr} \\ \tau_{rz} = G_s \gamma_{rz} \\ G_s = \frac{E_s}{2(1+\nu)} \end{cases} \tag{17}$$

where r_c is the radius of column inclusion, E_s and G_s are Young's modulus, and the shear modulus of the surrounding soil.

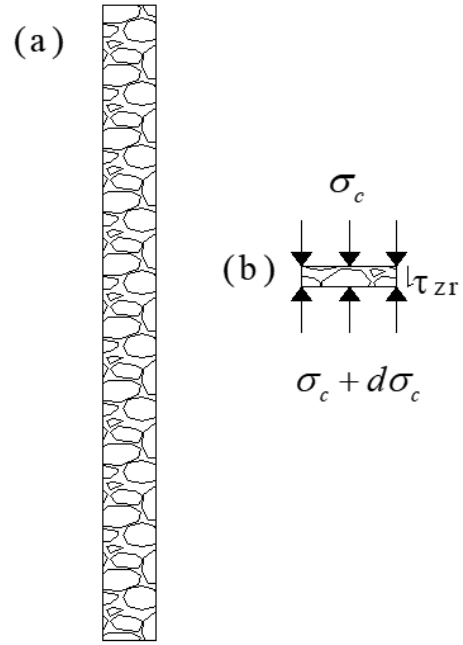

Figure 5. The unit cell of column inclusion: (**a**) sketch of the columnar inclusion, (**b**) force equilibriums for an element of the columnar inclusion.

Equation (17) can be re-written as the following equation:

$$\frac{d\sigma_c}{dz} = \frac{2G_s\dot{w}\phi}{r_c} \tag{18}$$

Substitute the boundary condition $\sigma_c^0 = \sigma_i$,

$$\sigma_c = \sigma_i + \frac{2aG_s\,h}{r_c\,\eta}\left[C_2\,I_1\,(a \times r_c) - C_1K_1\,(a \times r_c)\right]\left[coth(\eta) - \frac{cosh(\eta(1-\frac{z}{h}))}{sinh(\eta)}\right] \tag{19}$$

From Equation (19), the settlement of columnar inclusion can be obtained.

$$\begin{cases} S_c = \frac{\sigma_i h}{M_c} + \frac{2aG_s h^2}{r_c \eta M_c}(C_2 I_1(a \times r_c) - C_1 K_1(a \times r_c))(\cot(\eta) - \frac{1}{\eta}) \\ M_c = \frac{(1-\nu)E_c}{(1+\nu)(1-2\nu)} \end{cases} \tag{20}$$

It is assumed that there will be no slip happening between the column inclusion and the surrounding soil. Since the unit cell is symmetric, the following boundary conditions can be substituted into Equation (16):

$$\begin{cases} S_c = w(r_c) \\ \frac{dw}{dr}\Big|_{r=\frac{d_e}{2}} = a \times C_2 \times I_1(a \times \frac{d_e}{2}) - a \times C_1 \times K_1(a \times \frac{d_e}{2}) = 0 \end{cases} \tag{21}$$

The coefficients C_1 and C_2 can be obtained from Equation (21) (the detail can be seen in Appendix A) and the deformation of the surrounding soil can be derived.

3. Comparison with the Finite Element Method

To verify the newly proposed method, the finite element method (FEM) is used as a baseline. By comparing the calculated ground settlement between the FEM and the proposed method, the accuracy of the proposed method can be verified.

3.1. FEM Model

For the finite element analysis, the commercial software PLAXIS 2D (V22.02) is used. Based on the axisymmetric assumption, the mesh covering the solution regions is shown in Figure 6. The model was constructed using 822 15-noded triangular elements, and each element has 12 integration points at which the stress and strain are calculated. The load is divided into two parts, including σ_i = 1000 kPa, which acts as a uniform pressure on top of the column inclusions, and σ_o = 100 kPa, which is applied as a uniform pressure at the top of the surrounding soil. The boundary conditions of the FE model are consistent with those considered in the proposed theoretical method, that is, the base of the FE model is assumed to be rigid and therefore constrained vertically and horizontally, and the outer boundary is constrained in the horizontal direction and free in the vertical direction.

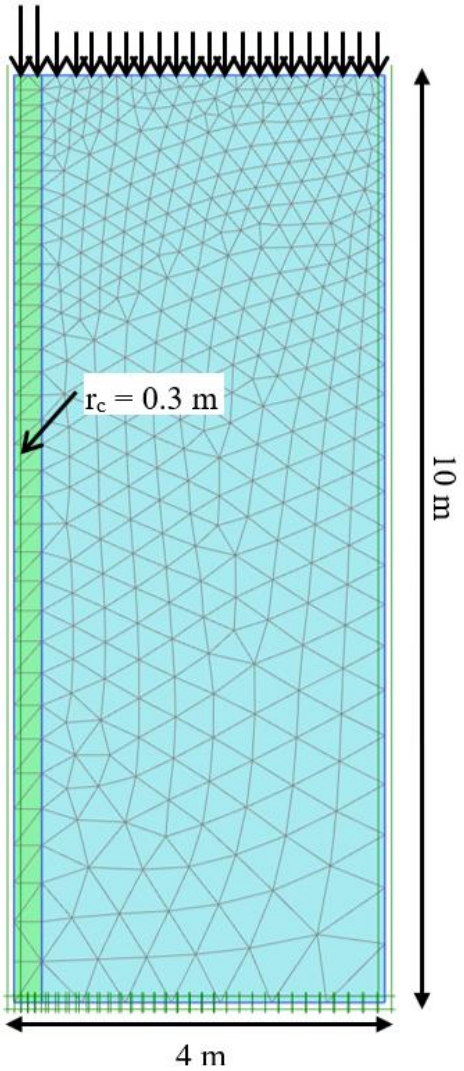

Figure 6. 2D axisymmetric finite element model for the unit cell.

In this FEM model, the surrounding soil and the columnar inclusion are assumed to be linear elastic. The values of the corresponding parameters are shown in Table 1.

Table 1. Material parameters of column inclusion and soil.

E_c (kPa)	ν_c	E_s (kPa)	ν_s
1,000,000	0.2	1000	0.4

3.2. Comparison with the Proposed Method

The settlement profiles of the ground surface along the radial distance calculated by Alamgir et al.'s [34] method, the FEM method, and the proposed method are plotted in Figure 7. As shown in this figure, there is a very good agreement between the predictions of the proposed method and the predictions of the FE analysis, although the proposed method slightly underestimates the predictions. The reason is that, for the proposed method, the pile is assumed to have only undergone axial compression, ignoring the axial shear deformation. In addition, the vertical displacement of the surrounding soil $\boldsymbol{W}$ is decomposed into the product of two univariate functions, which will decrease the degree of freedom of the model. However, for the FEM, with the number of elements used in this study, the model approaches the actual behavior, leading to larger predicted values of settlement. For the results coming from Alamgir et al.'s method, except that the settlement at the top of the column is close to that of the FEM solution, the estimated settlements of the surrounding soil are much larger than those calculated by the other two methods. The reason is that an over-simplified deformed shape function was adopted by Alamgir et al. As shown in this comparison, Alamgir et al.'s method gives overestimated settlement values for this case.

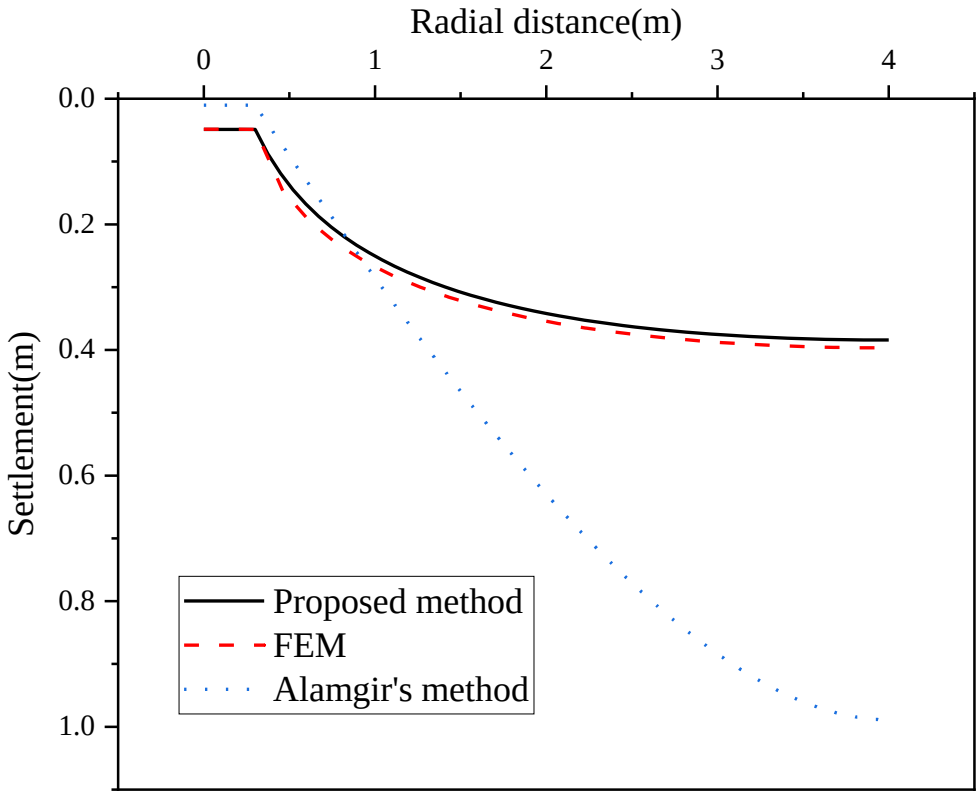

Figure 7. Settlement profile of the composite ground by three different methods.

4. Case History Study

Malekpoor and Poorebrahim [41] conducted a series of large-scale laboratory model experiments to explore the behavior of Compacted Lime-Well-graded Soil (CL-WS) rigid stone columns in soft soils. These tests were performed on composite specimens to evaluate the effect of different parameters, such as column diameter, slenderness ratio, area ratio, etc. To simulate the actual behavior of the CL-WS column-treated ground in the field, loads were applied over the entire area of the composite specimen to evaluate the increase in stiffness of the treated ground. When the entire area is loaded, settlement levels up to 15 mm were achieved at the top of the unit cell confinement, as shown in Figure 8.

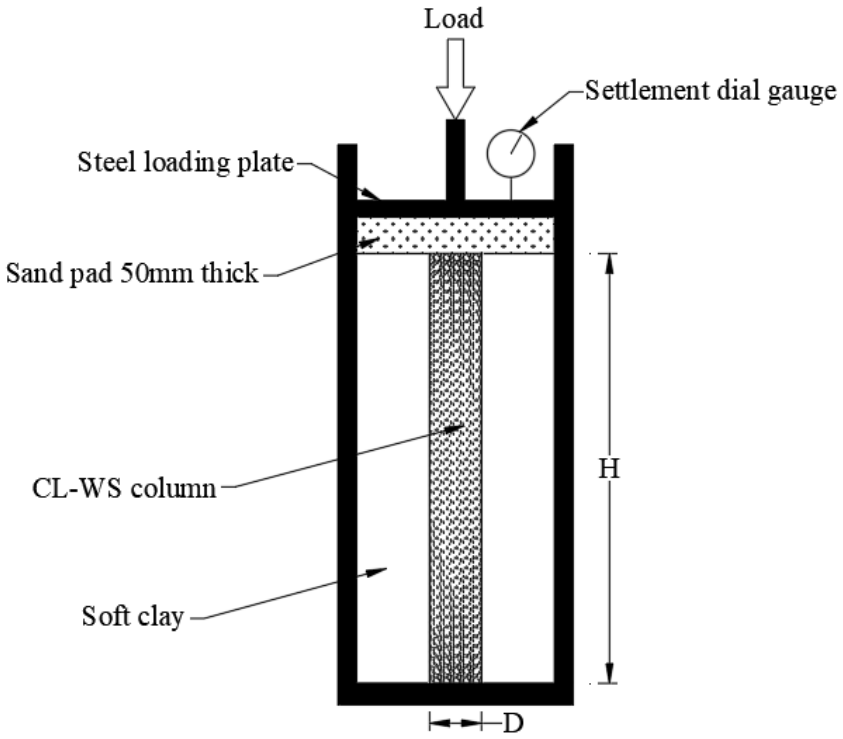

Figure 8. Laboratory test setups.

The properties of the soil and the columns were well recorded. However, the properties of the sand pad were not provided. When simulating the performance of column-reinforced soil using the proposed model, the deformation of the sand pad cannot be ignored. However, the deformation of the sand pad in the proposed method is relatively small since the sand is assumed to be in one-dimensional compression, and the stiffness of sand is assumed to be relatively large while the thickness is very small. The parameters of sand were calibrated from the back-analysis of the experiment. The properties of the materials are shown in Table 2.

Table 2. Physical and mechanical properties of materials used.

Material	E (kPa)	ν
Clay	12,000	0.41
Sand	20,000	0.3
Column	200,000	0.21

Firstly, the effect of the slenderness ratio, *H/D*, (the ratio between length, *H*, and diameter, *D*, of column) on the composite specimens is compared, as shown in Figure 9.

The results of laboratory model experiments, the proposed method, and FEM are quantitatively compared regarding the settlement up to 15 mm corresponding to the load intensity in the laboratory tests for different slenderness ratios. The results from the finite element analyses and experiments are very close, with differences ranging from 9.4 to 12%. This dissimilarity arises probably due to the overestimation of the stiffness of the sand pad. Throughout the derivation, the soil layer was assumed to be homogeneous and isotropic. This assumption no longer holds due to the presence of the sand pad. At the same time, the deformation of the sand pad cannot be ignored. Therefore, the deformation of the sand pad is assumed to be axial compression deformation, which increases the stiffness of the sand pad, resulting in the calculated settlements of the proposed method being smaller than those of the FEM and the experiments.

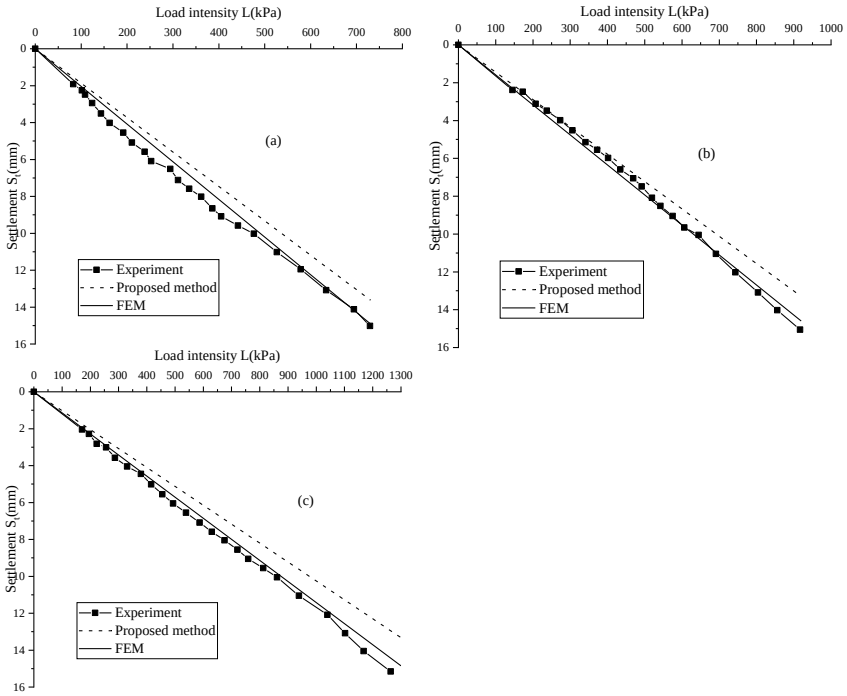

Figure 9. Effect of the slenderness ratio on the load intensity—settlement of composite specimens: (**a**) *H/D* = 8, (**b**) *H/D* = 6, (**c**) *H/D* = 4 (for 10% area ratio between the area of the column (Ac) and the total area within the unit cell (A) of 10%, and 100 mm column diameter).

The experimental procedure was also extended to evaluate the effect of model size on CL-WS column performance by changing the column diameter from 50 mm to 150 mm. Figure 10 shows the relationship between load intensity L and settlement S_t of a column with an area ratio equal to 10% and H/D = 6. A comparison of the results shows that the differences between them vary from 5.5% to 17%.

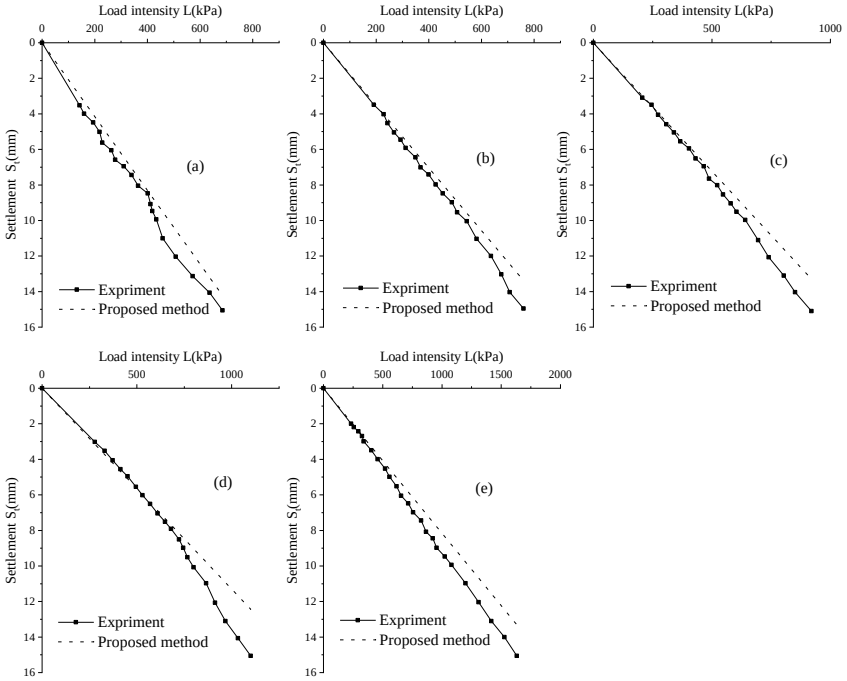

Figure 10. Effect of the diameter of the column on the load intensity—settlement of composite specimens: (**a**) *D* = 150 mm, (**b**) *D* = 125 mm, (**c**) *D* = 100 mm, (**d**) *D* = 75 mm, (**e**) *D* = 50 mm.

Figure 11 shows the variation of load intensity L versus settlement S_t for different area ratios, H/D = 6 and D = 100 mm. A comparison of the results reveals that the differences between them vary from 0.02 to 21.2%. With increasing area ratios, the difference decreases gradually.

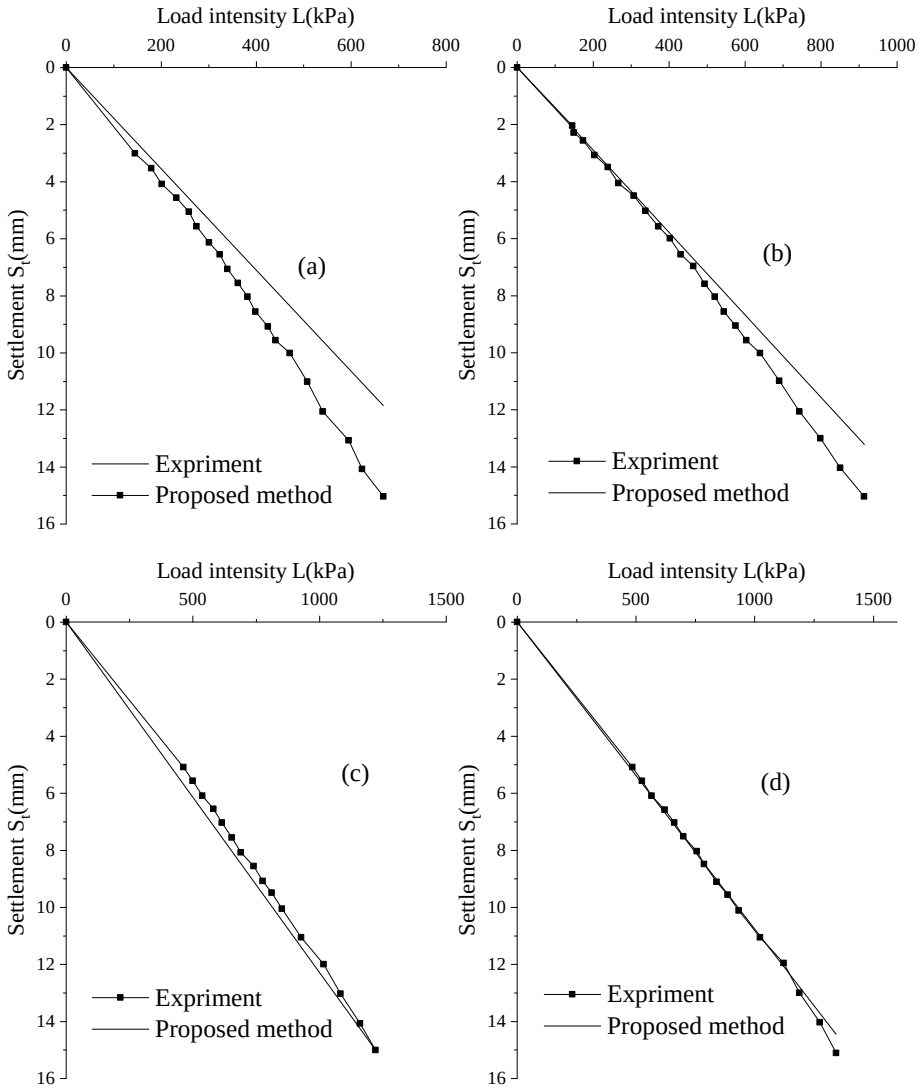

Figure 11. Effect of the area ratio (Ar) on the load intensity-settlement of composite specimens: (**a**) Ar = 5%, (**b**) Ar = 10%, (**c**) Ar = 15%, (**d**) Ar = 20%.

5. Parametric Study

For the fully penetrated column foundation, there are two key parameters influencing the settlement, including the ratio of elastic modulus between the column and the surrounding soil, E_c/E_s, the ratio between the radius of the column, and the radius of the model $r_c/(d_e/2)$. To study the effect of these parameters on the ground settlement, a series of parametric studies were conducted. The properties of the column and the surrounding soil are shown in Table 3. The pressure on the surrounding soil, σ_s, is 500 kPa, and the pressure on the stone column, σ_c, is 4000 kPa.

Figure 12 shows the ground settlement profiles for the fully penetrated column with various elastic modulus ratios. With an increasing elastic modulus ratio, the ground settlement becomes smaller. However, with the rate of the elastic modulus ratio increasing faster, the rate of settlement decrease becomes slower. In addition, by increasing the elastic modulus ratio, the supporting effect from the column to the soil becomes weaker as the settlement level increases more with the distance from the column.

Table 3. The reference parameters.

Material	Property	Value
Surrounding soil	Modulus of elasticity, E_s: kPa	4000
	Poisson's ratio, ν_s:	0.3
Stone column	Modulus of elasticity, E_c: kPa	400,000
	Poisson's ratio, ν_c:	0.2
	Length, H: m	10
	Radius of stone column, r_c: m	0.3
	Radius of model, $d_e/2$: m	5

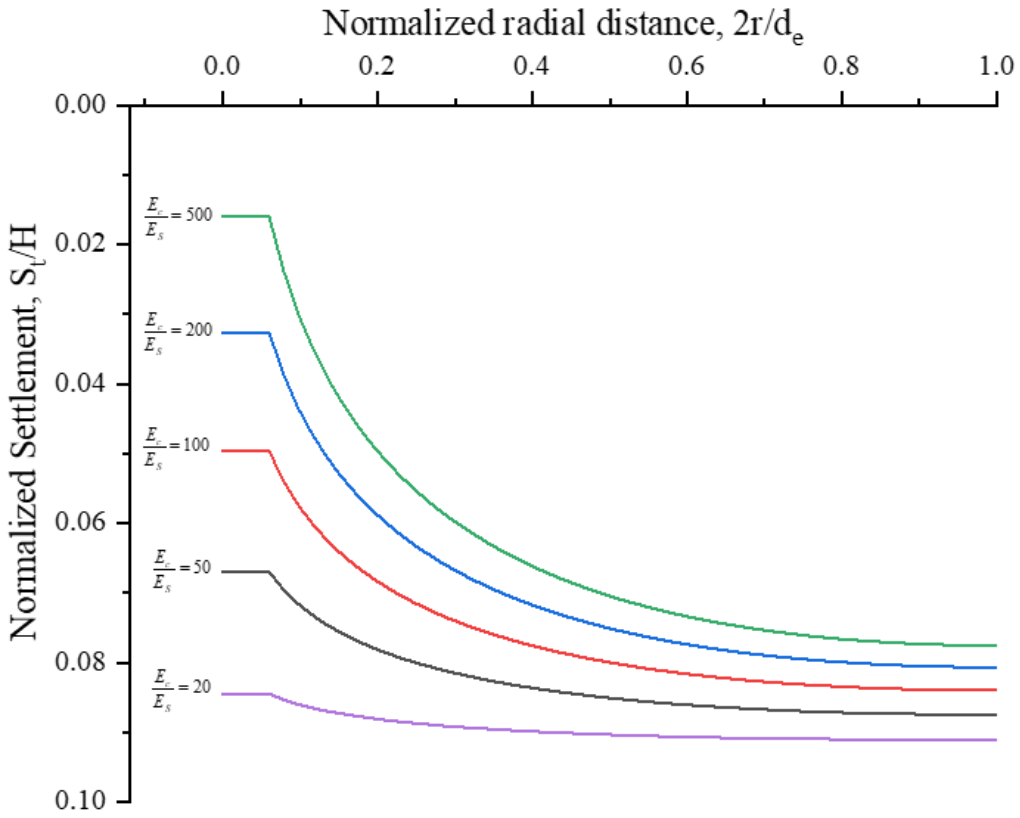

Figure 12. Ground settlement of the unit cell for the fully penetrated column with various elastic modulus ratios.

Figure 13 shows the ground settlement profiles for the fully penetrated column with various ratios between the radius and the spacing of the columns. With the increasing ratio between the radius and the spacing of the columns, the ground settlement becomes smaller. However, contrary to the previous phenomenon, the supporting effect is more obvious as the settlement does not increase with distance as much as in Figure 12.

The Poisson's ratio of the soil also plays an important role in the ground settlement of the column-reinforced foundation. As shown in Figure 14, the Poisson's ratio has a very big impact on the ground settlement. With an increase in Poisson's ratio of soil, the ground settlement decreases very quickly.

Compared with the Poisson's ratio of the soil, the Poisson's ratio of the column has a smaller effect on the ground settlement, as shown in Figure 15. The reason is that the area replacement ratio is only 0.36%. Therefore, the changing of the Poisson's ratio of the column produces a much smaller effect. With the increase in the area replacement ratio, the effect of Poisson's ratio of the column will be more pronounced.

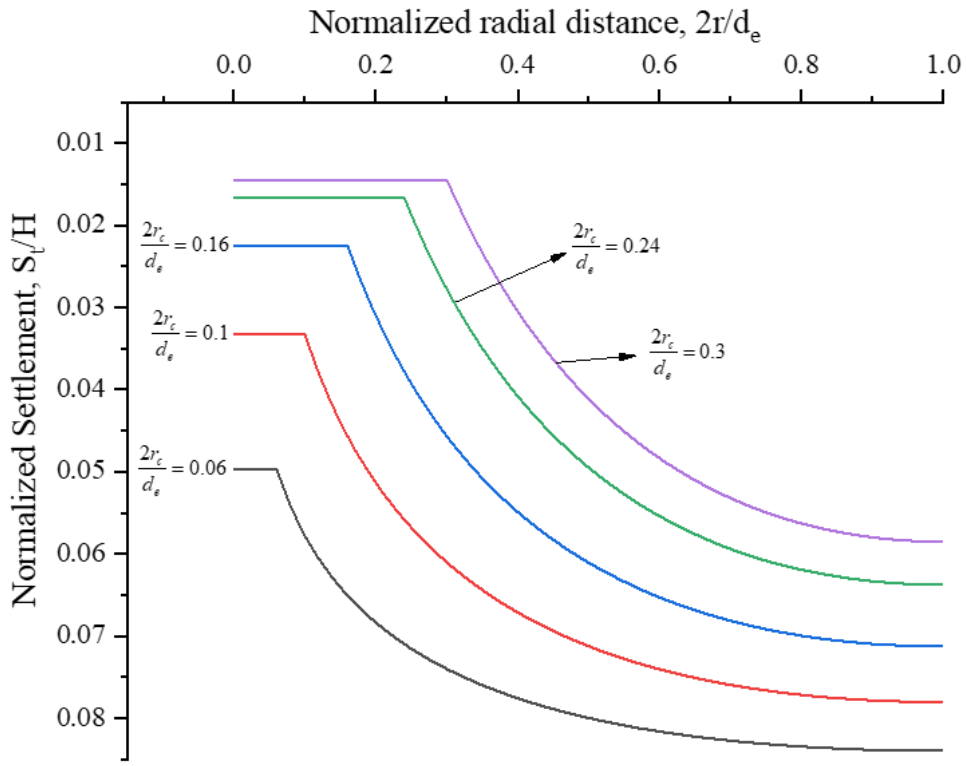

Figure 13. Ground settlement of the unit for the fully penetrated column with various ratios between the radius and the spacing of columns.

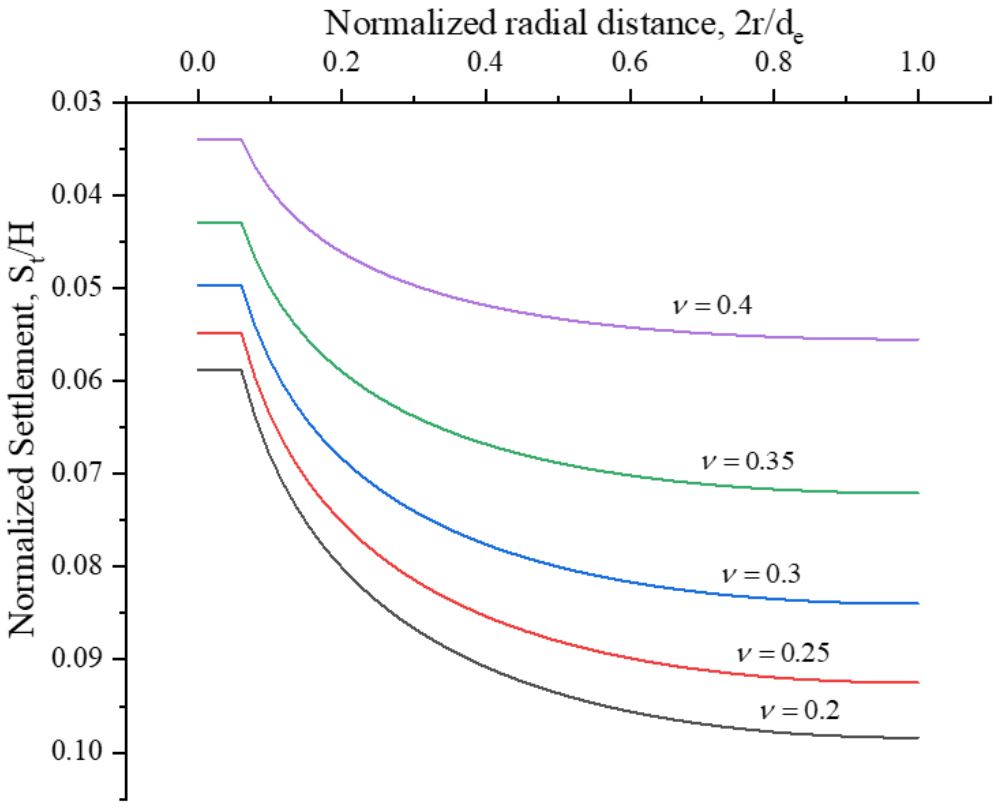

Figure 14. Ground settlement of the unit cell for the fully penetrated column with different Poisson's ratios of the soil.

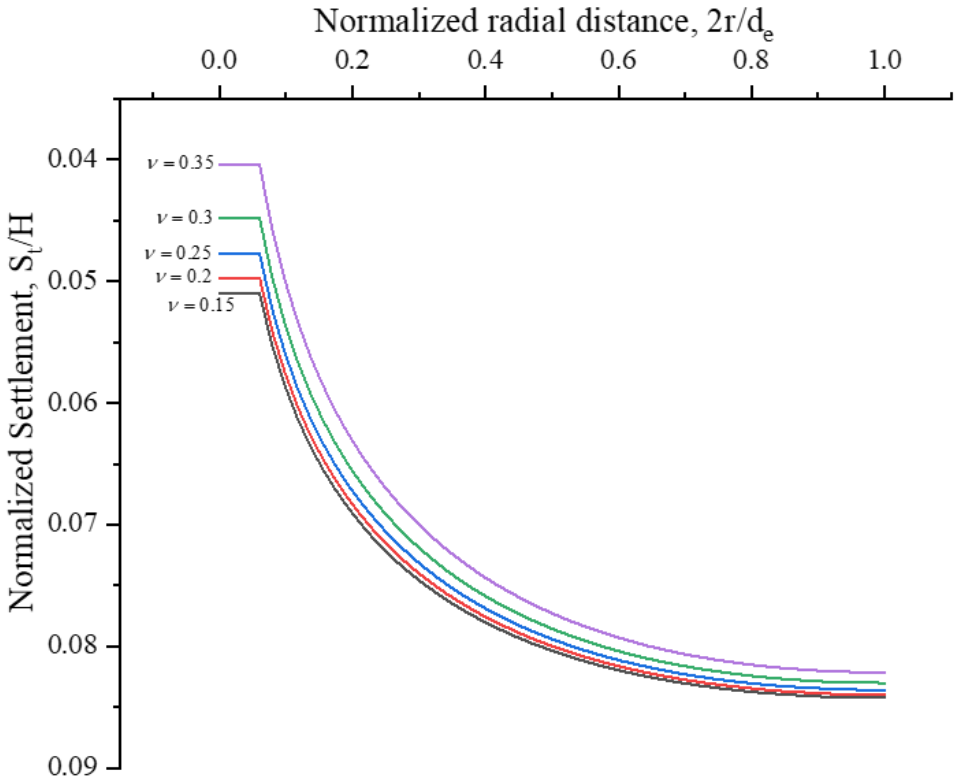

Figure 15. Ground settlement of the unit cell for the fully penetrated column with different Poisson's ratios of the column.

According to the previous results, with increasing Young's modulus and Poisson's ratio, the ground settlement decreases. The reason is that, for the limited lateral deformation and mainly the deformation caused by axial compression, the constraint modulus plays a major role.

$$M = \frac{E(1-\nu)}{(1+\nu)(1-2\nu)} \tag{22}$$

From Equation (22), the constraint modulus is a monotonically increasing function with respect to Young's modulus and Poisson's ratio as shown in Figure 16. With increasing Young's modulus and Poisson's ratio of surrounding soils and columns, the corresponding constraint modulus of surrounding soils and columns increases, which leads to the increasing axial stiffness of the model and, therefore, reducing deformation.

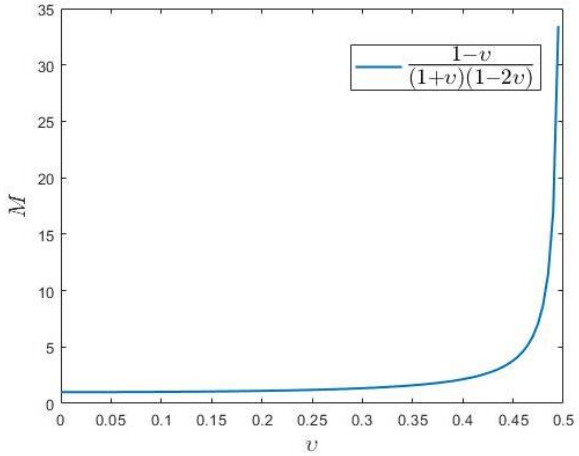

Figure 16. The relationship between constraint modulus M and Poisson's ratio υ.

The equivalent diameter of, d_e, of the unit cell also influences the ground settlement, and the corresponding results are shown in Figure 17. As shown in the figure, increasing d_e by 10% will produce a 12% increase in deformation.

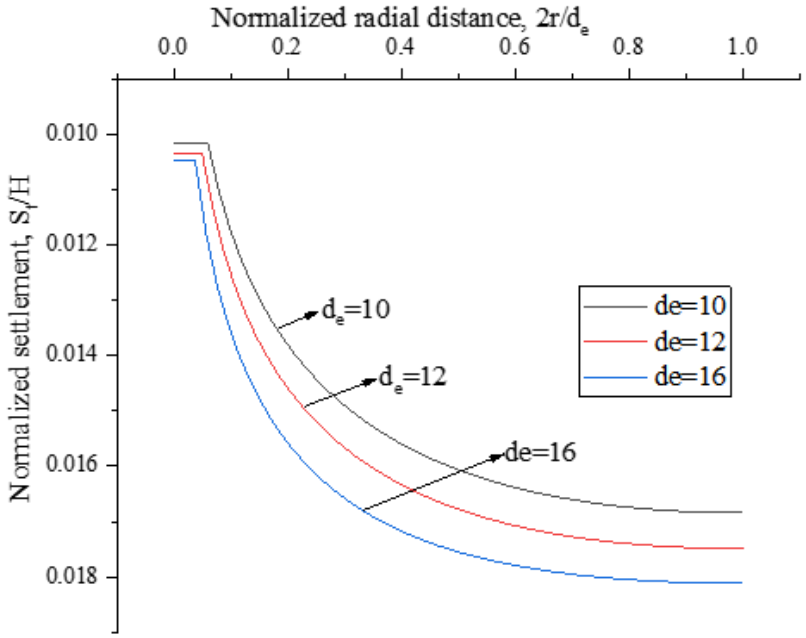

Figure 17. Ground settlement of the unit cell for the fully penetrated column with different equivalent diameter d_e.

6. Conclusions

In this study, a new method to calculate the ground settlement of column-reinforced foundations is proposed based on the variational principles. Compared with a previous empirical method, the proposed method has better physical meanings, and the derivation strictly follows the theory of the variational principle. Consequently, this method can be applied to a larger range of soil and column properties, as well as geometries in real practice. By comparing the finite element results and experimental data, it is verified that this method provides relatively accurate results.

In addition, a parametric study is presented to show the effects of influencing factors. From the study, by increasing the elastic modulus ratio between the column and the surrounding soil, and the ratio between the radius and the spacing of the stone columns, the supporting effect has been significantly improved, and the ground settlement becomes smaller. Furthermore, the equivalent diameter also affects the ground settlement, and with increasing the equivalent diameter, the ground settlement will increase accordingly. However, increasing the elastic modulus ratio between the column and the surrounding soils can only decrease the ground settlement close to the column, and the supporting effect becomes less as the distance from the column increases. In contrast, by increasing the ratio between the radius and the spacing of the columns, the overall settlement can be effectively reduced. In addition, the Poisson's ratio of the surrounding soil has a very significant effect on ground settlement. Compared with the soil, the effect of the Poisson's ratio of the column on the ground settlement can be ignored because the area replacement ratio is very small.

The proposed method is a basic model that, in future work, the researchers could combine with other superstructures, for example, embankments, to form a more comprehensive system. With this system, other factors, such as soil arching and stress intensity, can be further explored.

Author Contributions: Conceptualization, T.M.-H.L. and Z.Z.; methodology, T.M.-H.L. and Z.Z.; software, Z.Z.; validation, Z.Z.; formal analysis, Z.Z.; writing—original draft preparation, Z.Z.; writing—review and editing, T.M.-H.L. and L.-S.Z.; supervision, T.M.-H.L.; funding acquisition, W.-H.Z.; All authors have read and agreed to the published version of the manuscript.

Funding: The financial support for this study was provided through the research grant No.0035/2019/A1 from the Science and Technology Development Fund, Macau SAR, and the assistantship from the Faculty of Science and Technology, University of Macau.

Institutional Review Board Statement: Not applicable.

Informed Consent Statement: Not applicable.

Data Availability Statement: The data used in this study are available from the corresponding author upon reasonable request.

Conflicts of Interest: The authors declare no conflict of interest.

Appendix A

For the coefficients, C_1 and C_2 in Equation (16), by substituting the boundary condition in Equation (21) into Equation (16), the following equation can be derived:

$$\begin{cases} C_1(K_0(a*r_c) - b*I_1(a*r_c)) + C_2(I_0(a*r_c) + b*K_1(a*r_c)) = \frac{\sigma_i h}{M_c} - \frac{\sigma_o}{k} \\ -a*C_1*K_1(a*\frac{d_e}{2}) + a*C_2*I_1(a*\frac{d_e}{2}) = 0 \\ b = \frac{2aG_s h^2}{r_c \eta M_c} * (\cot(\eta) - \frac{1}{\eta}) \end{cases} \tag{A1}$$

At the same time, the functions $w(r)$ and $\phi(z)$ are coupled together. To decouple these two functions, the initial value of η can be assumed, then the shape function $\phi(z)$ can be obtained using Equation (14). The next step is to substitute the shape function into Equation (9), then the m and n can be represented by η.

$$\begin{cases} k = \frac{(1-\nu_s)E_s\eta*(\sinh(\eta)*\cosh(\eta)+\eta)}{2(1+\nu_s)(1-2\nu_s)H\sinh(\eta)^2} \\ G = \frac{E_s H(\sinh(\eta)*\cosh(\eta)-\eta)}{4(1+\nu_s)\sinh(\eta)^2\eta} \end{cases} \tag{A2}$$

The coefficient, a, will then be obtained. By substituting the a and η into Equation (A1), the coefficients, C_1 and C_2 will be obtained.

The above procedure needs just one iteration. If a more precise result is to be obtained, the updated function $w(r)$ may be substituted into Equation (11). By using Equation (12) to update η, the error between the updated η and previous η can be calculated. The iteration will be terminated when the error meets the threshold.

References

1. Manohar, R.; Patel, S. Ground Improvement with Stone Columns—A Review. In *Advances in Civil Engineering*; Springer: Singapore, 2021.
2. Singh, I.; Sahu, A. A Review on Stone Columns used for Ground Improvement of Soft Soil. In Proceedings of the of the 4th World Congress on Civil, Structural, and Environmental Engineering (CSEE'19), Rome, Italy, 7–9 April 2019.
3. Mohapatra, S.R.; Rajagopal, K.; Sharma, J. Direct shear tests on geosynthetic-encased granular columns. *Geotext. Geomembr.* **2016**, *44*, 396–405. [CrossRef]
4. Basack, S.; Indraratna, B.; Rujikiatkamjorn, C. Modeling the Performance of Stone Column–Reinforced Soft Ground under Static and Cyclic Loads. *J. Geotech. Geoenvironmental Eng.* **2016**, *142*, 04015067. [CrossRef]
5. Ghosh, B.; Fatahi, B.; Khabbaz, H.; Nguyen, H.H.; Kelly, R. Field study and numerical modelling for a road embankment built on soft soil improved with concrete injected columns and geosynthetics reinforced platform. *Geotext. Geomembr.* **2021**, *49*, 804–824. [CrossRef]
6. Dar, L.A.; Shah, M.Y. Accuracy analysis of 2D numerical methods of deep-seated failure analysis in embankments on stone column reinforced ground. *Innov. Infrastruct. Solut.* **2021**, *7*, 86. [CrossRef]
7. Chen, J.-F.; Li, L.-Y.; Zhang, Z.; Zhang, X.; Xu, C.; Rajesh, S.; Feng, S.-Z. Centrifuge modeling of geosynthetic-encased stone column-supported embankment over soft clay. *Geotext. Geomembr.* **2021**, *49*, 210–221. [CrossRef]

8. Pereira, P.G.d.S.; Pacheco, M.P.; Lima, B.T. Numerical analysis of soft soil improved with stone column technique. *REM-Int. Eng. J.* **2021**, *74*, 319–327. [CrossRef]
9. Mohapatra, D.; Kumar, J. Homogenization based kinematic limit analysis for finding the stability of an embankment over soft clay reinforced with granular columns. *Comput. Geotech.* **2022**, *142*, 104562. [CrossRef]
10. You, S.-K.; Lee, J.; Gabr, M.A. Experimental evaluation of recycled aggregate porous concrete piles for soft ground improvement. *Mar. Georesources Geotechnol.* **2016**, *34*, 712–720. [CrossRef]
11. Fahmi, K.S.; Kolosov, E.; Fattah, M.Y. Behavior of Different Materials for Stone Column Construction. *J. Eng. Appl. Sci.* **2019**, *14*, 1162–1168.
12. Aslani, M.; Nazariafshar, J.; Ganjian, N. Experimental Study on Shear Strength of Cohesive Soils Reinforced with Stone Columns. *Geotech. Geol. Eng.* **2019**, *37*, 2165–2188. [CrossRef]
13. Mehrannia, N.; Nazariafshar, J.; Kalantary, F. Experimental investigation on the bearing capacity of stone columns with granular blankets. *Geotech. Geol. Eng.* **2018**, *36*, 209–222. [CrossRef]
14. Chen, J.-F.; Wang, X.-T.; Xue, J.-F.; Zeng, Y.; Feng, S.-Z. Uniaxial compression behavior of geotextile encased stone columns. *Geotext. Geomembr.* **2018**, *46*, 277–283. [CrossRef]
15. Dash, S.K.; Bora, M.C. Bora, Improved performance of soft clay foundations using stone columns and geocell-sand mattress. *Geotext. Geomembr.* **2013**, *41*, 26–35. [CrossRef]
16. Bong, T.; Kim, S.-R.; Kim, B.-I. Prediction of Ultimate Bearing Capacity of Aggregate Pier Reinforced Clay Using Multiple Regression Analysis and Deep Learning. *Appl. Sci.* **2020**, *10*, 4580. [CrossRef]
17. Dar, L.A.; Shah, M.Y. Three Dimensional Numerical Study on Behavior of Geosynthetic Encased Stone Column Placed in Soft Soil. *Geotech. Geol. Eng.* **2021**, *39*, 1901–1922. [CrossRef]
18. Piccinini, I. *Ground Improvement with Stone Columns—Methods of Calculating Settlement Improvement Factor*; University of Glasgow, School of Engineering: Glasgow, UK, 2015.
19. Abhishek, S.V.; Rajyalakshmi, K.; Madhav, M.R. Engineering of ground with granular piles: A critical review. *International J. Geotech. Eng.* **2016**, *10*, 337–357. [CrossRef]
20. Castro, J.; Cimentada, A.; da Costa, A.; Cañizal, J.; Sagaseta, C. Consolidation and deformation around stone columns: Comparison of theoretical and laboratory results. *Comput. Geotech.* **2013**, *49*, 326–337. [CrossRef]
21. Çadır, C.C.; Vekli, M.; Şahinkaya, F. Numerical analysis of a finite slope improved with stone columns under the effect of earthquake force. *Nat. Hazards* **2021**, *106*, 173–211. [CrossRef]
22. Tang, L.; Cong, S.; Ling, X.; Lu, J.; Elgamal, A. Numerical study on ground improvement for liquefaction mitigation using stone columns encased with geosynthetics. *Geotext. Geomembr.* **2015**, *43*, 190–195. [CrossRef]
23. Castro, J. An analytical solution for the settlement of stone columns beneath rigid footings. *Acta Geotech.* **2016**, *11*, 309–324. [CrossRef]
24. Deb, K. Modeling of granular bed-stone column-improved soft soil. *Int. J. Numer. Anal. Methods Geomech.* **2008**, *32*, 1267–1288. [CrossRef]
25. Sexton, B.G.; McCabe, B.A.; Castro, J. Appraising stone column settlement prediction methods using finite element analyses. *Acta Geotech.* **2014**, *9*, 993–1011. [CrossRef]
26. Aboshi, H.; Ichimoto, E.; Enoki, M.; Harada, K. The Compozer—A Method to Improve Characteristics of Soft Clays by Inclusion of Large Diameter sand Columns. In Proceedings of the International Conference on Soil Reinforcements: Reinforced Earth and Other Techniques, Paris, France, 20–22 March 1979; pp. 211–216.
27. Chow, Y.K. Settlement Analysis of Sand Compaction Pile. *Soils Found.* **1996**, *36*, 111–113. [CrossRef]
28. Balaam, N.P.; Booker, J.R. Analysis of rigid rafts supported by granular piles. *Int. J. Numer. Anal. Methods Geomech.* **1981**, *5*, 379–403. [CrossRef]
29. Balaam, N.P.; Booker, J.R. Effect of stone column yield on settlement of rigid foundations in stabilized clay. *Int. J. Numer. Anal. Methods Geomech.* **1985**, *9*, 331–351. [CrossRef]
30. Priebe, H.J. The design of vibro replacement. *Ground Eng.* **1995**, *28*, 31.
31. Pulko, B.; Majes, B. Simple and Accurate Prediction of Settlements of Stone Column Reinforced soil. In *Proceedings of the 16th International Conference on Soil Mechanics and Geotechnical Engineering*; IOS Press: Amsterdam, The Netherlands, 2005.
32. Zhang, L.; Zhao, M.; Shi, C.; Zhao, H. Settlement Calculation of Composite Foundation Reinforced with Stone Columns. *Int. J. Geomech.* **2013**, *13*, 248–256. [CrossRef]
33. Zhao, L.-S.; Zhou, W.-H.; Yuen, K.-V. A simplified axisymmetric model for column supported embankment systems. *Comput. Geotech.* **2017**, *92*, 96–107. [CrossRef]
34. Alamgir, M.; Miura, N.; Poorooshasb, H.; Madhav, M. Deformation analysis of soft ground reinforced by columnar inclusions. *Comput. Geotech.* **1996**, *18*, 267–290. [CrossRef]
35. Deb, K.; Mohapatra, S.R. Analysis of stone column-supported geosynthetic-reinforced embankments. *Appl. Math. Model.* **2013**, *37*, 2943–2960. [CrossRef]
36. Zhao, L.-S.; Zhou, W.-H.; Geng, X.; Yuen, K.-V.; Fatahi, B. A closed-form solution for column-supported embankments with geosynthetic reinforcement. *Geotext. Geomembr.* **2019**, *47*, 389–401. [CrossRef]
37. Tanahashi, H. Pasternak Model Formulation of Elastic Displacements in the Case of a Rigid Circular Foundation. *J. Asian Archit. Build. Eng.* **2007**, *6*, 167–173. [CrossRef]

38. Vallabhan, C.V.G.; Das, Y.C. Parametric Study of Beams on Elastic Foundations. *J. Eng. Mech.* **1988**, *114*, 2072–2082. [CrossRef]
39. Jones, R.; Xenophontos, J. The Vlasov foundation model. *Int. J. Mech. Sci.* **1977**, *19*, 317–323. [CrossRef]
40. Vlasov, V.Z. Beams, plates and shells on elastic foundation. *Isr. Program Sci. Transl.* **1966**. Available online: https://scirp.org/reference/referencespapers.aspx?referenceid=577015 (accessed on 22 September 2022).
41. Malekpoor, M.R.; Poorebrahim, G. Behavior of Compacted Lime—(Well-graded) Soil columns: Large scale tests and numerical modelling. *KSCE J. Civ. Eng.* **2014**, *19*, 893–903. [CrossRef]